ACS OMEGA

Open Access

http://pubs.acs.org/journal/acsodf

Article

Development of Nanofluid-Based Solvent as a Hybrid Technology for In-Situ Heavy Oil Upgrading During Cyclic Steam Stimulation Applications

Hugo Alejandro García-Duarte, María Carolina Ruiz-Cañas, Henderson Quintero, Oscar E. Medina, Sergio H. Lopera, Farid B. Cortés, and Camilo A. Franco*

Cite This: *ACS Omega* 2024, 9, 40511−40521

Read Online

ACCESS | Metrics & More | Article Recommendations

ABSTRACT: This paper evaluates solvent-based nanofluids for in situ heavy oil upgrading during cyclic steam stimulation (CSS) applications. The study includes a comprehensive analysis of the properties and characteristics of nanofluids, as well as their performance in in situ upgrading and oil recovery. The evaluation includes laboratory experiments to investigate the effects of the nanoparticle's chemical nature, asphaltene adsorption and gasification, heavy oil recovery, and quality upgrading. The results show that alumina-based nanoparticles have a higher efficiency in asphaltene adsorption and catalytic decomposition at low temperatures (<250 °C) than ceria and silica nanoparticles. Specifically, alumina nanoparticles achieved asphaltene adsorption of 48 mg g^{-1}, while ceria adsorbed 42 mg g^{-1}. Alumina and ceria required around 90 and 135 min for 100% asphaltene conversion. Nanofluids were designed by varying nanoparticle and surfactant concentrations dispersed in naphtha, obtaining that the nanofluid containing 0.05 wt % of nanoparticles and 0.05 wt % of surfactant presents the highest yield in increasing API gravity by 5° and reducing oil viscosity by 90% in thermal experiments. Finally, the nanofluid was evaluated under dynamic conditions. The results show that nanofluid-based solvents can significantly improve the recovery and upgrading of heavy oil during CSS applications. When the steam injection technology was assisted by naphtha and nanofluid, 64% and 75% of the original oil in place were recovered, respectively. The effluents obtained in each stage presented lower API gravity values and higher viscosities for those obtained without a nanofluid. Specifically, the API gravity of the recovered oil rose from 11.9° to 34°, and the viscosity decreased to below 100 cP. The paper concludes by highlighting the potential of nanofluid-based solvents as a promising technology for heavy oil recovery and upgrading in the future.

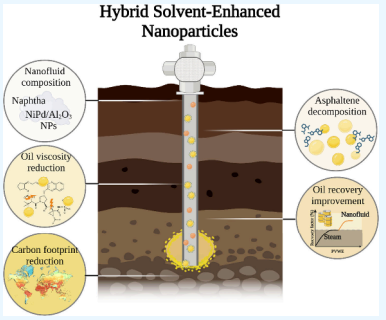

1. INTRODUCTION

Colombia's oil production is predominantly characterized by heavy crude oils, constituting approximately 45% of the current production.[1] This implies a big challenge due to the elevated amount of heavy fractions, including asphaltenes and resins, inherently present in these crude oils. Hence, their extraction may include heat injection into the reservoir through thermal-enhanced oil recovery (TEOR) methods, including oil combustion, steam injection, and microwave heating. These methods have been widely studied with different degrees of success.[2,3] Oil combustion, or in situ combustion (ISC), ignites a portion of the oil in the reservoir to generate heat, reducing the remaining oil's viscosity and making it easier to extract. This method is effective but can be challenging to control and may result in incomplete combustion.[3] Microwave heating, on the other hand, uses electromagnetic waves to directly heat the oil.[2] This method offers precise control over the heating process and can achieve rapid temperature increases but requires specialized equipment and may have limitations in terms of penetration depth. Steam injection emerged as a prominent process designed to reduce heavy oil viscosity. Despite its efficacy, the typical recovery factors for steam injection range between 50% and 60%.[4] Also, the substantial energy requirements inherent in steam injection processes and escalating energy consumption costs require innovative solutions. Current challenges include significant heat losses and the need for natural gas to generate steam. Recognizing the imperative requirement for sustainable alternatives that minimize the carbon footprint, this study delves into hybrid technologies.[4,5]

Among the innovative approaches, applying solvents with cyclic steam injection has emerged as a promising approach. Specifically, integrating metallic nanoparticles into organic solvents, known as nanoparticle-enhanced solvents (or hybrid

Received: April 11, 2024
Revised: September 3, 2024
Accepted: September 6, 2024
Published: September 16, 2024

solvent-enhanced nanoparticles—Hyb-SEN), represents a pioneering concept. Hyb-SEN offers the prospect of enhancing crude oil properties through catalytic reactions, such as aquathermolysis, inherent in steam injection.

Nanotechnology plays a pivotal role in catalyzing reactions for asphaltene thermal decomposition, representing a transformative avenue for heavy oil recovery. Asphaltenes, known for their complex molecular structures, pose a significant challenge in conventional extraction processes.[6] Integrating metallic nanoparticles, precisely engineered at the nanoscale, introduces a catalytic process. These nanoparticles act as catalysts, facilitating the breakdown of complex asphaltene molecules through enhanced surface interactions.[5,7] The unique catalytic properties at the nanoscale accelerate the thermal decomposition of asphaltenes during steam injection and contribute to upgrading crude oil properties. This innovative approach addresses the viscosity-related challenges inherent in heavy oils and opens new horizons for the efficient recovery of valuable hydrocarbons.[8]

For instance, Afzal et al.[9] investigated the application of Fe_2O_3 and WO_3 nanoparticles in coreflooding experiments to enhance heavy oil recovery during steam injection. Their results demonstrated significant improvements in oil recovery and viscosity reduction, highlighting the potential of the nanoparticle-assisted EOR method. Hamedi et al.[10] explored the use of nickel nanoparticles in coreflooding tests, showing enhanced oil displacement and in situ upgrading effects during steam injection. Additionally, Franco et al.[11] conducted coreflooding experiments using silica nanoparticles doped with 1 wt % Ni and Pd, demonstrating improved oil recovery and reduced oil viscosity under steam injection conditions. Furthermore, Cardona et al.[12,13] investigated the performance of doped alumina nanoparticles with Ni and Pd to assist a steam injection test by varying steam quality, showing significant improvements in oil recovery and asphaltene decomposition. Lastly, Medina et al.[14,15] examined using ceria nanoparticles functionalized with Ni and Pd in coreflooding experiments, achieving enhanced oil recovery and improved thermal stability during steam injection, as an upgraded heavy crude oil with 99% reduced viscosity.

Implementing displacement tests is inherently tied to assessing the success and efficiency of the nanotechnology-assisted steam injection process for heavy oil recovery.[16] These tests serve as crucial benchmarks, offering tangible insights into the effectiveness of the technology. Moreover, these tests enable the identification of optimal injection strategies, helping refine the application of the technology in real-world scenarios.[14,15]

This paper serves as a critical juncture in advancing the understanding and application of hybrid technologies, presenting experimental results on the characterization and evaluation of nanomaterials pivotal to the Hyb-SEN methodology. The insights derived from this study lay the groundwork for subsequent numerical simulations, aiming to discern the most optimal injection strategy for implementation in the field. By shedding light on the intricate interplay between nanotechnology and steam injection, the study expands the theoretical foundation and paves the way for practical implementations that could redefine the landscape of heavy oil recovery, offering sustainable and efficient solutions for the challenges unique to Colombia's oil industry.

2. MATERIALS AND EQUIPMENT

Alumina nanoparticles doped with nickel and palladium (AlNP) were supplied by a local company, and ceria nanoparticles doped with nickel and palladium (CeNP) were supplied by Fenómenos de Superficie Research group (Universidad Nacional de Colombia). Ten nm Alumina nanoparticles (Al_2O_3-γ) were supplied by NanoAmor (Texas, USA) and were used to synthesize Ni (1%)-functionalized (HCS) and Ni (1.3%)-functionalized (HCM) alumina nanoparticles. Nickel nitrate hexahydrate (Merck Millipore, Burlington, MA, USA) was used to synthesize the HCS and HCM using the incipient wetness technique. A Colombian heavy oil, *n*-heptane (C_7H_{16}, 100%, Sigma-Aldrich, St. Louis, MO, USA), naphtha, with an API of 64°, and deionized water were used for static and dynamic tests.

Different steps in the experimental procedure employed reservoir fluids, specifically heavy oil and brine, provided by a Colombian oil company. Table 1 provides a summary of the crude oil's properties. The API gravity was determined using the ASTM D-1250 standard, while the SARA fractionation adhered to the IP 469 standard, employing a TLC-FID/FPD Iatroscan MK6 instrument (Iatron Laboratories Inc., Tokyo, Japan). NaCl, $CaCl_2{\cdot}2H_2O$, $MgCl_2{\cdot}6H_2O$, $BaCl_2{\cdot}2H_2O$, and KCl, all sourced from Sigma-Aldrich (St. Louis, MO, USA), were employed for brine preparation. The isolation of asphaltenes was performed according to the ASTM D2892 and ASTM D5236 standards.[17]

Table 1. Main properties of heavy crude oil

Properties		Heavy oil
API ° ± 1°		11.9
Viscosity 25 °C (cP) ± 100 cP		39140
SARA content	Saturates (%) ± 0.3%	19.0
	Aromatic (%) ± 0.3%	47.2
	Resins (%) ± 0.3%	32.0
	Asphaltenes (%) ± 0.7%	1.80

Sand samples obtained from Ecopetrol S.A. (Colombia) were used to construct the porous media, following a previously described method.[13] Porous media cleaning was performed using methanol (99.8%), toluene (99.8%), and HCl (37%), all sourced from Merck KGaA (Darmstadt, Germany).[13,18]

3. METHODS

3.1. Synthesis of Nanoparticles. Al-10-HCS and Al-10-HCM syntheses were performed using the incipient wetness technique.[19] This method consists of preparing an aqueous solution with a Ni salt (Ni^{2+} and a "volatile" anion such as chloride, nitrate, acetate, or carbonate) and slowly adding it to the support until only the void volume (pores) of the latter is filled. The water and anion are subsequently removed in the drying and calcination stage, which leads to the oxidation of the Ni ions present (NiO) on the support surface.[20] The nanomaterial synthesis methodology was based on the proposals by Franco et al.[21] and González, Mutiz, and Urrest,[22] which consists of drying the support nanoparticles at a temperature of 120 °C for 2 h. Subsequently, they are impregnated with an aqueous solution of Ni salts ($NiCl_2{\cdot}6H_2O$) and palladium if desired for 3 h. The HCM nanoparticle has a higher concentration of nickel chloride in its preparation, so it is expected to have a higher concentration

https://doi.org/10.1021/acsomega.4c03517
ACS Omega 2024, 9, 40511−40521

of nickel on its surface than HCS, specifically 1.3 wt % ± 0.5 wt % for the HCM and 1 wt % ± 0.5 wt % for HCS nanoparticle.

Finally, the material is dried at 120 °C and subsequently calcined at 450 °C to deposit the oxides of metallic nanoparticles on the surface of the support nanoparticles.

3.2. Characterization of Nanoparticles. Nanoparticle mean size was determined through dynamic light scattering (DLS) using a NanoPlus (Micromeritics, USA) at room temperature. Samples were dispersed in deionized water (50 mg/L) and sonicated for 2 h. The hydrodynamic average diameter of the nanoparticles at room temperature is calculated by the Stokes−Einstein equation. The size of the nanoparticles was also corroborated by Transmission Electron Microscopy (Eindhoven, The Netherlands). The nanoparticles were dispersed in solutions with pH values between 2 and 12 units to measure the isoelectric point. To achieve this, solutions prepared with NaOH (1.0 M) and HCl (0.1 M) were adjusted with a digital pH meter D-50 (Horiba, Japan). Each dispersion was taken to NanoPlus 3 equipment (Micromeritics, USA) to measure the zeta potential. The following techniques were applied to characterize the active phases on the nanoparticles. Inductively coupled plasma mass spectrometry (ICP−MS) was employed to evaluate the content of Ni and/or Pd nanoparticles based on the procedure described in a previous work.[8] The dispersion of the metals in the catalyst support was determined through pulse chemisorption and H_2 titration with a Chembet 3000 (Quantachrome Instruments, Boynton Beach, FL, USA). Approximately 100 mg of the sample was dried at 200 °C in a U-shaped quartz tube for one hour. Following a one hour exposure to 600 °C at 80 mL min^{-1} of 10%H_2/Ar, the catalysts were reduced. Then, the samples were purged in an Ar atmosphere for an additional hour. Finally, H_2 pulses persisted until no more H_2 uptake was detected.

3.3. Adsorption Tests and Catalytic Decomposition Analysis for Nanoparticle Selection. The adsorption capacity of the nanoparticles for asphaltenes was determined by constructing adsorption isotherms. Oil model solutions with varying asphaltene concentrations (100 mg·L^{-1}−2000 mg·L^{-1}) were prepared by diluting in toluene. The equipment and protocol for constructing the adsorption isotherms are detailed in previous studies.[15,23,24]

The noncatalytic and catalytic decomposition of asphaltenes was assessed by thermogravimetric analysis at reservoir pressure (700 psi) using an HP-TGA 750 (TA Instruments Inc., Hüllhorst, Germany). The experiments were conducted under isothermal steam injection conditions (250 °C) for 300 min. Details of the procedures can be found in a previous study.[25]

3.4. Nanofluid Design. The nanoparticle dosage was determined through crude oil upgrading tests. For this purpose, naphtha was mixed with varying concentrations of the top two nanoparticles at levels of 0, 500, 1000, and 2000 mg L^{-1}. During these tests, mixtures of heavy oil and 5 wt % naphtha + nanoparticles were made. In these tests, heavy oil was combined with a 5 wt % mixture of naphtha and nanoparticles. The mixtures were mechanically stirred to ensure a complete dilution of the nanofluid in the crude oil. The prepared systems were placed in a reactor set to a temperature of 250 °C, replicating the conditions of the steam injection test. The systems were heated for 5 h and then cooled under an ice bath at 2 °C to condense the light compounds. Subsequently, the samples were characterized for API gravity and dynamic viscosity. The thermal conductivity of the nanofluids was analyzed with a TEMPOS thermal properties analyzer (Meter, USA), following ASTM 5334 and IEEE 442 standards. The equipment was previously calibrated with glycerin, and the measurements were carried out in triplicate to ensure repeatability.

3.5. Oil Recovery and Upgrading Tests. For dynamic tests, two different porous media were used. Porous medium 1 and 2 were used for determining the potential of naphtha and nanofluid in oil recovery, respectively. The porosity of the medium was measured via a saturation method. At the same time, permeability was calculated using Darcy's law.[13,18] Table 2 shows the absolute and oil-effective permeabilities for both systems.

Table 2. Basic characteristics of porous media

Properties	Porous Medium 1	Porous Medium 2
Mineralogy	Silica (99%)	Silica (99%)
Porosity (%) ± 0.2%	25.6	25.9
Pore Volume (cm^3) ± 3 cm^3	212	203

The displacement tests were conducted in three phases to simulate the field conditions for steam injection. Steam, at 70% quality and 250 °C, was used in the tests, with steam quality verified through numerical simulation following protocols from previous studies.[13,15] In the first phase, steam was injected at rates between 3 and 5 mL min^{-1} until crude oil production ceased. The second phase involved estimating the incremental crude oil produced by injecting either naphtha or nanofluid in liquid form, with injection rates ranging from 0.5 mL·min^{-1} and 1 mL·min^{-1}. The third phase began once no further increase in oil production was noted; the porous media were allowed to rest for 12 h, after which steam injection resumed until oil production stopped. Throughout the process, the pressure profile was monitored to ensure the effective transport of naphtha and nanofluids within the steam stream.

The overburden pressure and pore pressure were fixed at 2000 and 150 psi, respectively. The details of the displacement system can be found in previous publications.[13−15] Different thermocouples were also located in the porous medium to determine the temperature drop. For both experiments (without and with a nanofluid), the temperature was maintained between 250 and 230 °C from the inlet to the outlet of the sample holder.

After the tests, the crude oil recovered was characterized by SARA distribution, API gravity, and dynamic viscosity in an Anton Paar Stabinger SVM 3000 (Madrid, Spain).[12,26] Details of the protocols are described elsewhere.[13,14] The persistence of the treatment's effect on crude oil quality was assessed by monitoring API gravity and dynamic viscosity over four consecutive weeks.

4. RESULTS AND DISCUSSION

The results of the characterization and evaluation of nanomaterials proposed for the implementation of a hybrid technology of solvent-enhanced nanoparticles (Hyb-SEN) with CSS are shown in this section.

4.1. Characterization of Nanoparticles. Initially, a state-of-the-art analysis of nanoparticles and nanocomposites that could have catalytic effects in steam injection processes was carried out. From that, asphaltenes were classified according to their viscosity reduction, decomposition temperature reduc-

https://doi.org/10.1021/acsomega.4c03517
ACS Omega 2024, 9, 40511−40521

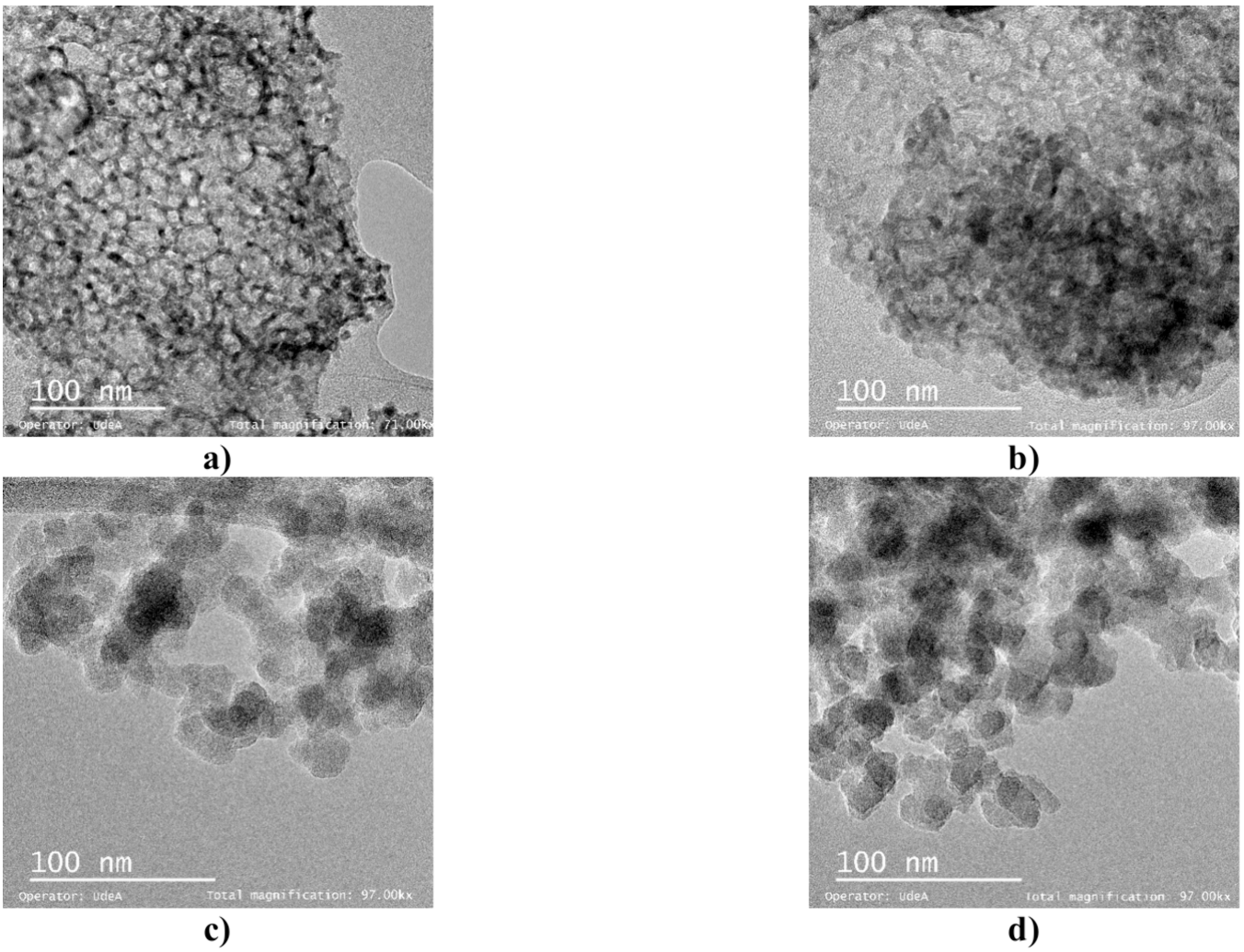

Figure 1. Micrographs of (a) AlNP, (b) AlNP, (c) CeNP, and (d) Al-10-HCS nanoparticles.

tion, and conversion properties, as well as an increase in the recovery factor, which generally refers to their catalytic performance in steam injection processes, especially in aquatermolysis reactions.[27] Figure 1 shows micrographs of three nanomaterials AlNP, CeNP, and Al-10−1HCS. The micrographs show materials in nanometric size, circular form, but irregular structures that form networks with pore spaces. Also, TEM micrographs show areas of higher-resolution contrastable black regions that are attributable to metals on the surface, which corroborates the presence of nickel and palladium in its structure. Also, this technique corroborates the nanometer size of the structures.

It highlights that restricting the particle size to nanometric conditions is essential for reservoir applications to avoid formation damage. On the other hand, knowing the physicochemical characteristics of nanocatalysts allows for analyzing the relationship between the catalytic performance of materials and their chemical nature.

Likewise, Table 3 shows the particle size, isoelectric point, and metal dispersion. The results reveal the nanometric conditions of all materials with sizes smaller than 100 nm and isoelectric points close to 7 for most cases. However, the HCM nanoparticle has a surface chemistry prone to acidity (isoelectric point of 5.4). On the other hand, the highest metal dispersion was obtained by the CeNP nanoparticle

Table 3. Physicochemical properties of AlNP, CeNP, HCS, and HCM nanocatalysts[a]

Sample	Hydrodynamic Radius (nm)	Isoelectric Point	Dispersion of Metals (%)
AlNP	76.0 ± 2.0	7.7 ± 0.2	29 ± 1.5
CeNP	20.2 ± 0.9	7.5 ± 0.2	32 ± 1.2
Al-10-HCS	67.0 ± 0.5	7.1 ± 0.2	0.8 ± 0.1
Al-10-HCM	90.0 ± 0.5	5.4 ± 0.2	7.6 ± 0.1

[a]Hydrodynamic diameter was measured through dynamic light scattering, the isoelectric point was measured by zeta potential measurements, and metal dispersion was measured by H_2 titration.

(32%), followed by the AlNP nanoparticle with a concentration of 29%. The total amount of Ni and Pd (determined by ICP-MS) was close to 1 wt.% for each element in CeNP and AlNP. In the case of Al-10-HCS and Al-10-HCM, the amount of nickel was 1 wt.% and 1.3 wt.%, respectively.

The inclusion of nanocatalysts enhances the heat conductivity of naphtha. Additionally, there exists a relationship between the metallic composition of the nanoparticles and their efficacy in facilitating heat conduction within the solvent. Table 4 illustrates the conductivities of the various nanomaterials investigated in naphtha at a concentration of 2000 ppm.

https://doi.org/10.1021/acsomega.4c03517
ACS Omega 2024, 9, 40511−40521

Table 4. Thermal conductivity for naphtha and naphtha enhanced with nanocatalysts

Sample	Thermal conductivity ($W \cdot mK^{-1}$) ± 0.001
Naphtha	0.1232
Naphtha/AlNP	0.2531
Naphtha/CeNP	0.2432
Naphtha/Al-10-HCS	0.1782
Naphtha/Al-10-HCM	0.1123

It is evident that the most efficient heat conduction is achieved with AlNP nanoparticles in a solvent resembling naphtha.

This outcome stems from the correlation between the heat conductivity and the presence of Nickel (Ni) and Palladium (Pd) metals on the surfaces of AlNP and CeNP. The more metallic nanoparticles present on the surface, the better the conduction of heat and electricity. This is facilitated by the free movement of electrons within the structural network created by Ni and Pd metals, which readily release electrons from their structures, transforming them into conductive cations. In contrast, nanoparticles like HCS and HCM, possessing solely nickel on their surfaces and a reduced metal concentration, exhibit a lower heat conductivity.

4.2. Static Evaluation of Nanoparticles. Figure 2a displays the adsorption isotherms constructed for *n*-C_7 asphaltenes on nanoparticles. The profiles of these isotherms, classified as type Ib according to the International Union of Pure and Applied Chemistry (IUPAC), align well with previously reported results, which describe the adsorption of asphaltenes on nanometric solid surfaces.[28] Generally, asphaltene adsorption was marginally higher on AlNP nanoparticles and comparable to that on CeNP. These findings suggest a strong affinity of asphaltenes for the metallic phases of Ni and Pd, with a slightly higher affinity for alumina-based species compared with ceria-based ones. Alumina (Al_2O_3) and ceria (CeO_2) have different surface chemistries. The chemical groups and functional sites on the surface of alumina may be more conducive to forming favorable interactions with asphaltenes than ceria. The specific adsorption sites on alumina might offer stronger binding sites for asphaltene molecules. As reported by Nassar et al.[29] asphaltene adsorption on alumina nanoparticles is spontaneous and exothermic in nature, obtaining the equilibrium adsorption in less than 2 h. In another study, Lopes et al.[30] proved that the enthalpy of adsorption of model asphaltenes on alumina is higher than on untreated samples as a result of the availability of a higher number of energetic sites. In general, several authors recommended alumina for asphaltene adsorption.[31−33,21,34]

Considering the reservoir conditions characterized by high temperatures and pressures, the alumina nanoparticles maintain their structural integrity and surface reactivity. The elevated temperatures enhance the mobility of asphaltene molecules, increasing the likelihood of their contact with the nanoparticles. Moreover, the high pressure helps maintain the nanoparticles' dispersion stability within the oil matrix, ensuring a uniform distribution throughout the reservoir.[35]

Figure 2b shows the isothermal thermogravimetric analysis of asphaltenes adsorbed and nonadsorbed over nanoparticles at high pressure. AlNP decomposes 100% of both adsorbed asphaltenes at a lower time than CeNP, AL-10−1HC, and Al.-10-HCM, in that order. AlNP required around 90 min for asphaltene conversion. Finally, for the Al-10-HCS material, despite converting asphaltenes to a greater extent compared to the scenario without nanoparticles, conversion was below 40% in the entire evaluated time range.

Based on the discoveries, Figure 3 illustrates a potential reaction pathway for asphaltene interacting with the ceria nanocatalyst. The process seems to involve the fragmentation of heavy compounds, facilitated by the cleavage of alkyl chains or aromatic rings, yielding alkyl radicals (·R) and leading to the formation of CO by C-radical oxidation and the lattice oxygen of CeO_2 (resulting in the redox cycle of ceria). Alumina may exhibit a similar behavior through the oxidation of Al^{2+} to Al^{3+}. Subsequently, steam promotes the water−gas shift reaction (WGSR) on the catalyst's surface, converting oxygenated compounds into hydrogen. This in situ-generated hydrogen could facilitate hydrogenation or hydrocracking reactions of heavy hydrocarbons, including the hydrogenation of free radicals (·R) produced by thermal cracking with steam molecules, such as CAC cleavage, b-scission, isomerization, H-abstraction, and olefin addition. Alternatively, the mechanism might involve the cracking of an aliphatic chain, resulting in the formation of two free radicals: one in the aromatic nucleus and one in the aliphatic chain. If these free radicals manage to be stabilized by hydrogen molecules during the process, then both the aromatic nucleus and the aliphatic chain could be stabilized. Otherwise, the aromatic nucleus could combine with a similar fraction, leading to the formation of a

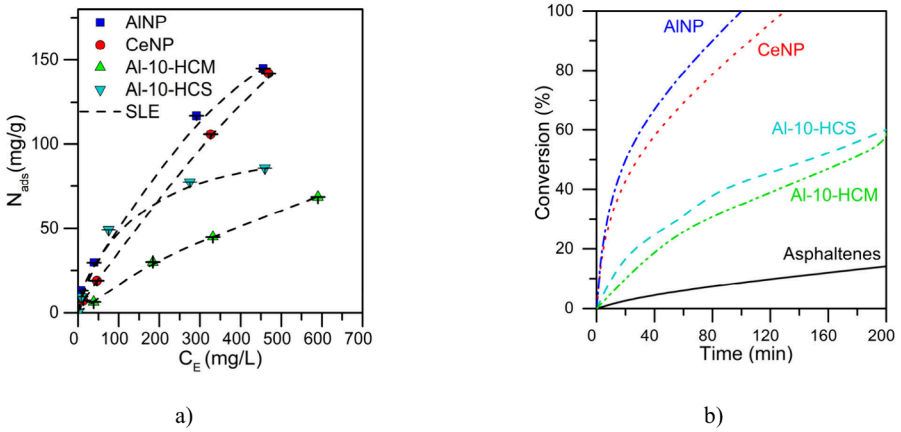

a) b)

Figure 2. (a) Asphaltene adsorption isotherms over different nanoparticles (dotted lines represent the SLE fitting) and (b) Isothermal conversion of asphaltenes under steam gasification in the absence and presence of nanoparticles.

https://doi.org/10.1021/acsomega.4c03517
ACS Omega 2024, 9, 40511−40521

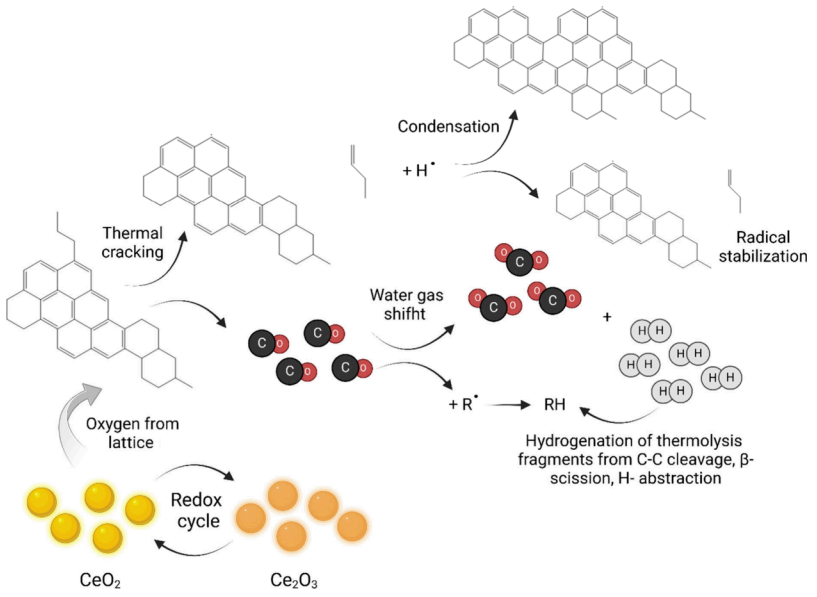

Figure 3. Schematic illustration of catalytic steam gasification of asphaltenes using ceria-based nanocatalysts.

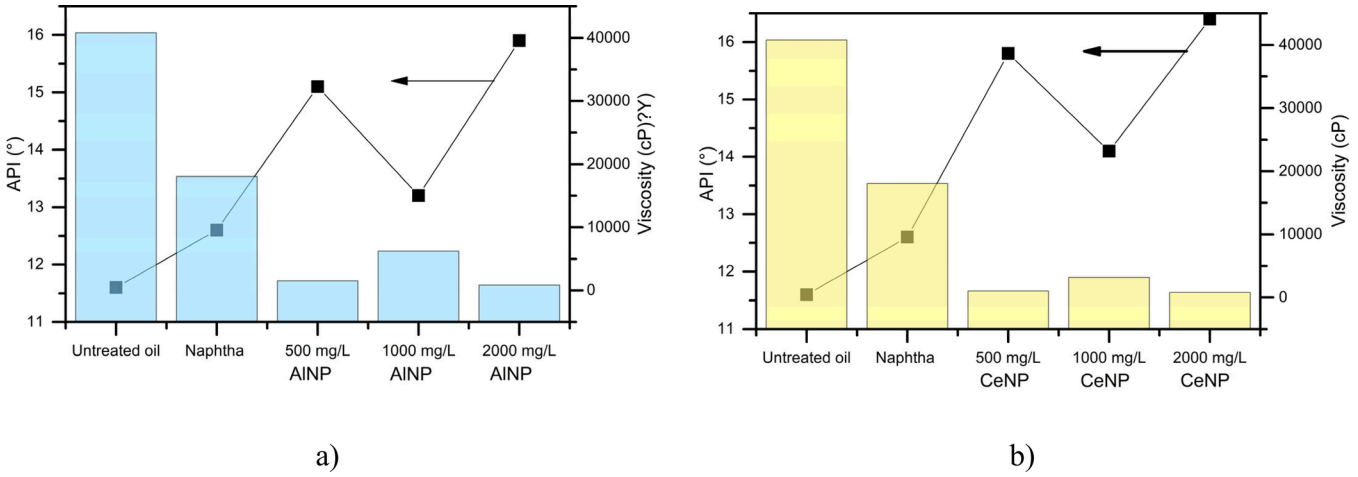

Figure 4. Crude oil properties (API gravity and dynamic viscosity) before and after treatment with nanofluid containing (a) AlNP and (b) CeNP nanoparticles.

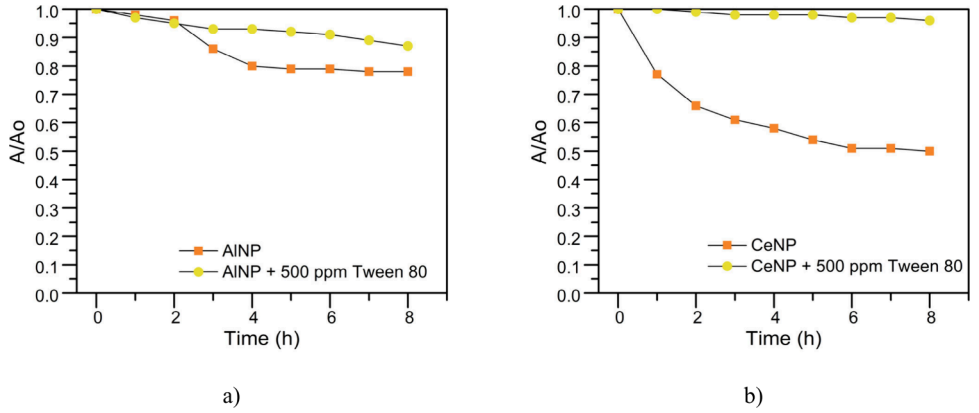

Figure 5. Absorbance ratio of mixtures of (a) AlNP and (b) CeNP nanoparticles dispersed on naphtha with and without Tween 80 surfactant as a function of sedimentation time.

more complex structure with a higher molecular weight through polycondensation. The proposed catalysts are anticipated to mitigate polycondensation, ultimately reducing the coke yield and increasing the yield of light oils. The required oxygen for the reaction is supplied through redox reactions, specifically Ce^{3+}-Ce^{4+} lattice oxygen, while the

https://doi.org/10.1021/acsomega.4c03517
ACS Omega 2024, 9, 40511−40521

regenerated catalyst can be reactivated with active oxygen from steam, thus enhancing catalytic stability. The catalyst regeneration process contributes to the generation of hydrogen from steam.

4.3. Nanofluid Design. AlNP and CeNP nanoparticles were selected for the formulation of two nanofluids, considering adsorption and catalytic experiments. The amount of nanoparticles was selected by breeding tests in a reactor and characterized by API gravity and dynamic viscosity. The concentration of each nanoparticle varied between 500 and 2000 mg·L^{-1}. Figure 4 shows the results of both properties for the evaluated systems. The first system analyzed was crude oil at 250 °C. This will be the baseline scenario to compare with those of the other systems. The naphtha system contains a mixture of crude oil and 5wt.% naphtha. In both systems, a reduction of more than 50% in the viscosity and a slight increase in the API gravity of the crude oil are obtained by using only naphtha. The other systems are a composition of crude oil with 5wt.% of naphtha and different concentrations of nanoparticles. For both systems, a better performance was obtained with the dosages of 500 and 2000 mg·L^{-1} in terms of both properties. Therefore, 500 mg·L^{-1} of AlNP and 500 mg·L^{-1} of CeNP were selected for the formulation of both nanofluids.

The nanofluids consisting of naphtha carrier fluid and 500 mg L^{-1} AlNP and CeNP nanoparticles were characterized by UV−vis to analyze their stability as a function of time. Figure 5 shows the results obtained from the relative absorbance.

Figure 5a shows that AlNP is the most stable sample with a 20% reduction at 8 h. Meanwhile, the CeNP mixture was less stable with A/Ao reduction to less than 50% after 8 h. To increase the stability of nanofluids, 500 mg·L^{-1} of Tween 80 was added, and the results evidenced an increase in the stability of around 90% in both cases, being slightly higher in AlNP than CeNP. Then, the nanofluid was formulated with naphtha containing 500 mg·L^{-1} of AlNP and 500 mg·L^{-1} of Tween 80 surfactant.

4.4. Coreflooding Test Steam Injection Assisted with Naphtha and Nanofluid. Figure 6a shows the oil recovery profiles from coreflooding tests. The measured absolute oil permeability was 1263 mD, and the effective oil permeability (ko) was 897 mD. During the initial steam injection, a 47% recovery was obtained. The mechanisms responsible for oil recovery during steam injection include the reduction of oil viscosity through heat transfer, thermal expansion of the oil, gravitational segregation of reservoir fluids, volatilization of lighter hydrocarbons, and the expansion of fluids and rock within the reservoir.[12,36] After the injection of the liquid naphtha batch and soaking for 12 h, an increase in recovered oil of 18% was obtained, indicating the potential of naphtha to assist this type of technology and provide higher oil recovery. Naphtha is expected to contribute to oil viscosity reduction and thermal expansion when assisting steam.

The oil recovery curve for steam injection assisted by the nanofluid consisting of 500 m mg·L^{-1} AlNP and 500 mg·L^{-1} Tween 80 dispersed in naphtha is shown in Figure 6b. These tests estimated the absolute and effective oil permeability (ko) at 1115 and 866 mD, respectively. After 9 pore volume wate equivalent (PVWE) was injected, a recovery of 51% of the oil is obtained. After the nanofluid injection, the recovery increases to 74%, representing an incremental of 24%. The better performance obtained when the technology is assisted by nanotechnology could be related to the fast interaction

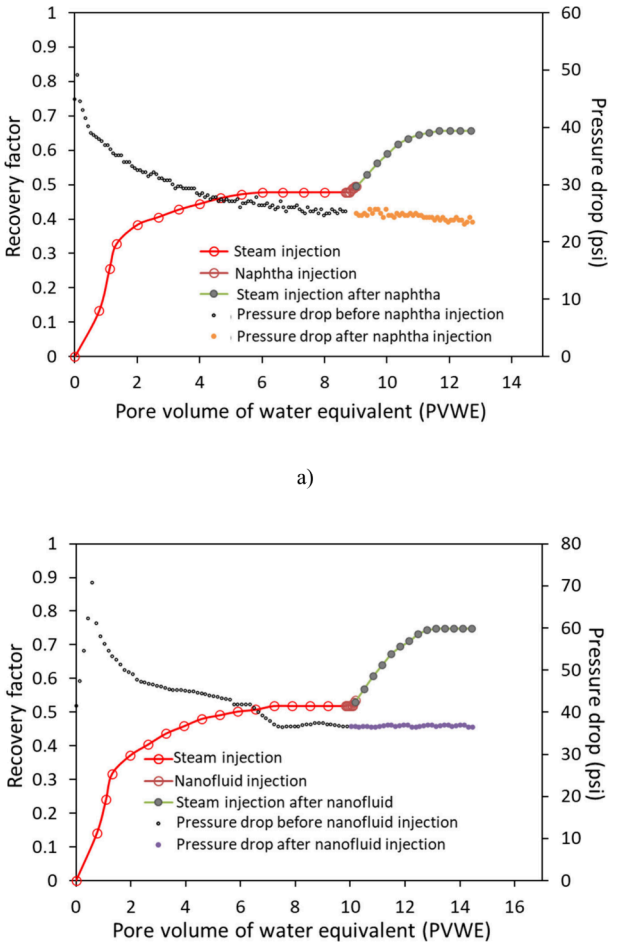

Figure 6. Oil recovery and pressure drop curves during steam injection with (a) naphtha and (b) nanofluid containing 500 mg·L^{-1} of AlNP.

between steam and the active sites of the alumina-, nickel-, and palladium-based nanoparticles.[16]

In addition, the rate of C−C bond breaking in the catalytic cracking of heavy oil fractions was improved, and higher amounts of H_2 and O_2 species could be produced from the splitting of steam molecules to stabilize free radicals from asphaltenes and resins and prevent the formation of more complex structures.[16] At the same time, the increase in asphaltene-Al_2O_3 interactions allowed greater oxygen adsorption and release.[37] Therefore, the oxygen anion vacancies on the nanocatalyst surface became unstable,[6,38] breaking down the heavy oil fractions by partial oxidation via nanocatalyst-promoted oxygen production or water via redox reaction.[39]

4.5. Effluent Analysis from Steam Injection Test. Figure 7a shows the API gravity and viscosity values for raw crude oil, crude oil after steam injection, and crude oil recovered during steam injection after naphtha injection. From the figure, the API gravity did not change during steam injection, remaining close to the value of untreated crude (11.9°). However, the viscosity decreased due to the heat transfer from the steam to the crude oil. That could also be related to the reduction of the cohesive forces on the molecular structures of the combined asphaltene-resin compounds. After the injection of naphtha, the API gravity increased to 20.9°, and the viscosity decreased to near 587 cP. This scenario is

https://doi.org/10.1021/acsomega.4c03517
ACS Omega 2024, 9, 40511−40521

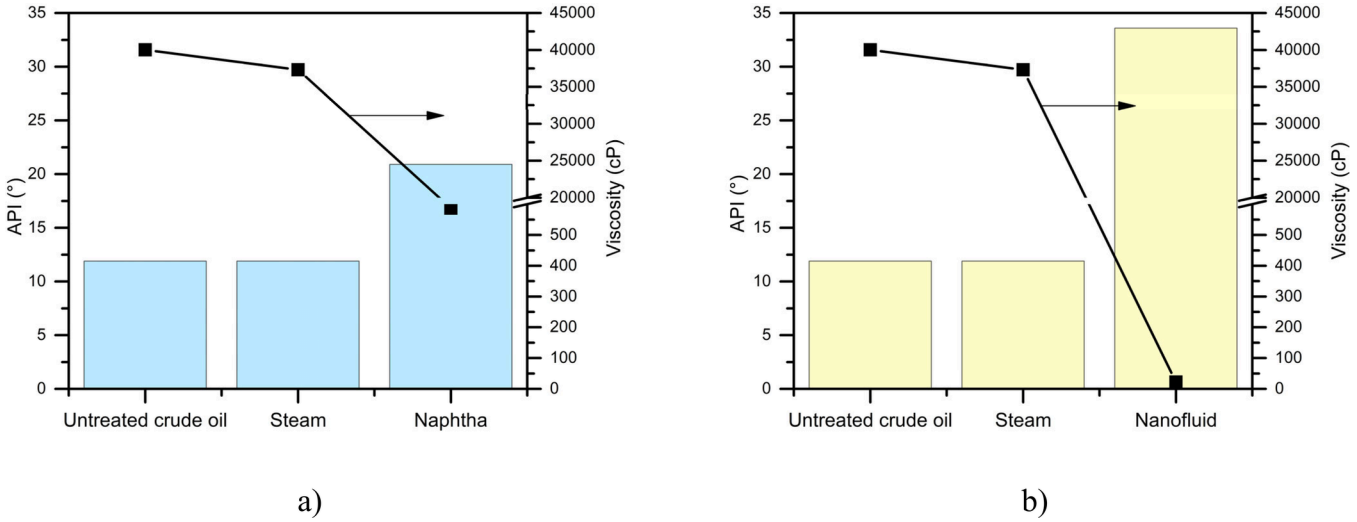

Figure 7. Crude oil properties (API gravity and viscosity) before and after the steam injection with (a) naphtha and (b) nanofluid containing 500 mg·L^{-1} of AlNP.

widely influenced by the dilution effects of naphtha in crude oil.

Figure 7b shows the changes in API gravity and viscosity of the samples recovered in the different phases of the displacement test. The API gravity of the crude oil remained stable at 11.9° poststeam injection, while its viscosity slightly dropped from 40,020 to 3,700 cP. However, with the introduction of nanofluid, the API gravity rose dramatically to 33°, and the viscosity significantly decreased to 22 cP. These results highlight the superior ability of nanoparticles to enhance crude oil quality compared to using naphtha alone. The improvements are due to several factors: the synergistic effect of metal oxides on nanoparticle surfaces,[40] strong metal support interactions,[23,41] and catalytic reactions that promote H_2 and radical stabilization.[42] These combined effects lead to a substantial reduction in heavy oil compounds, increased saturated components, and decreased aromatic structures.[39]

The effectiveness of alumina-based nanofluids for heavy oil recovery and upgrading has been a focal point of this study. The main conclusions derived from the experimental and analytical investigations indicate that alumina-based nanofluids significantly improve the thermal conductivity of the injected fluids. This enhancement facilitates more efficient heat transfer within the reservoir, resulting in better thermal propagation and improved oil recovery rates.[43,44] Additionally, introducing alumina nanoparticles into the heavy oil matrix effectively reduces the oil viscosity. This reduction can be associated with two main mechanisms. The first is related to disrupting the oil viscoelastic network formed by resins and asphaltenes as a result of nanoparticle affinity for these components.[45] This mechanism is the first responsible for reducing oil viscosity and improving its flow characteristics. The other mechanism is attributed to the catalytic effects of the nanoparticles, which promote the thermal decomposition of heavy fractions, such as asphaltenes and resins.

Furthermore, alumina nanoparticles act as catalysts for aquathermolysis reactions during steam injection. These reactions break down complex hydrocarbon molecules into simpler, lighter compounds, as described in the literature.[46−48] As a result, there is a noticeable improvement in the quality of the crude oil, with an increase in the API gravity and a decrease in the sulfur content. The synergistic effect of enhanced thermal conductivity, reduced viscosity, and catalytic upgrading contributes to a higher recovery efficiency.

Moreover, the assisted steam injection by naphtha and alumina nanoparticles resulted in a lower energy consumption and reduced operational costs. The reduced requirement for steam generation translates to savings in fuel costs and a smaller carbon footprint. A recent study explored the life-cycle assessment (LCA) of using alumina nanoparticles to assist steam injection in crude oil extraction.[49] The research focused on four scenarios: steam injection at 0.5 and 1.0 quality with and without 500 mg L^{-1} of alumina-based nanoparticles doped with Ni and Pd. The findings indicated that utilizing nanoparticles allowed for extracting higher energy-quality crude oil. The environmental impact analysis revealed that using steam injection at 1.0 quality with nanoparticles significantly reduced environmental impacts like marine ecotoxicity, urban land occupation, particulate matter formation, and global warming potential, demonstrating that nanoparticles are the best option in terms of LCA. They helped to achieve better energy and environmental performance, making them a viable and sustainable enhancement for crude oil recovery processes.[49] In summary, this study highlights the promising potential of alumina-based nanofluids as an advanced EOR technique. Their ability to enhance thermal efficiency, reduce oil viscosity, catalyze upgrading reactions, and improve overall recovery efficiency makes them a viable and sustainable solution for heavy oil recovery and upgrading.

The findings of this study have significant implications for field applications of hybrid technology using alumina-based nanofluids for heavy oil recovery and upgrading. The demonstrated enhancements in thermal conductivity and viscosity reduction suggest that when applied in the field, this technology can improve the efficiency of steam injection processes. This efficiency increase can lead to a more effective heat distribution within the reservoir, resulting in higher oil recovery rates and reduced operational costs.

The catalytic properties of alumina nanoparticles, which facilitate the thermal decomposition of heavy fractions, such as asphaltenes and resins, indicate that this technology can improve the quality of the extracted crude oil. This improvement could result in lighter, less viscous oil with a

https://doi.org/10.1021/acsomega.4c03517
ACS Omega 2024, 9, 40511−40521

higher API gravity and lower sulfur content, which is more desirable and valuable in the market.

Furthermore, the increased recovery efficiency and reduced steam requirements can lead to significant energy savings and a smaller environmental footprint. These benefits make the hybrid technology a more sustainable option for heavy oil recovery, aligning with the industry's growing emphasis on environmental responsibility and cost-effectiveness.

5. CONCLUSIONS

The HCS, HCM, AlNP, and CeNP materials are nanometric in size and have a considerable composition of metals on their surface, which is directly related to thermal conductivity, which is higher in all cases than the base fluid for naphtha preparation.

The AlNP nanofluid with 0.05 wt % of nanoparticles in naphtha presents the highest yield in increasing API gravity and reducing oil viscosity in thermal experiments.

The statics evaluation shows that AlNP nanoparticles have a higher efficiency in asphaltene adsorption and catalytic decomposition at low temperatures (<250 °C) concerning ceria nanoparticles.

Likewise, the TGA tests to evaluate the kinetics of asphaltene decomposition in the presence of nanomaterials show that the best catalytic performance was obtained with the nanomaterial AlNP (alumina-based nanoparticles with nickel and palladium), followed by CeNP (cerium-based nanoparticles with nickel and palladium), and finally by HCS; the latter presented two decomposition peaks, which is unfavorable for the cracking process due to the remnant of higher molecular weight asphaltenes.

According to the results obtained from the rock-fluid evaluation when the steam injection technology was assisted by naphtha and nanofluid, 64% and 75% of the original oil in place was recovered, respectively. The nanomaterial used for the evaluation with the highest catalytic performance named AlNP corresponds to nanoparticles of alumina (Al_2O_3) coated with nickel oxide (NiO) and palladium oxide (PdO). Also, the effluents obtained in each stage presented lower API gravity values and higher viscosities than those obtained without nanofluid, highlighting the potential of nanofluid-based solvents as a promising technology for heavy oil recovery and upgrading in the future.

AUTHOR INFORMATION

Corresponding Author

Camilo A. Franco − *Grupo de Investigación en Fenómenos de Superficie - Michael Polanyi, Departamento de Procesos y Energía, Facultad de Minas, Universidad Nacional de Colombia, Sede Medellín 050034, Colombia;* orcid.org/0000-0002-6886-8338; Email: caafrancoar@unal.edu.co

Authors

Hugo Alejandro García-Duarte − *ECOPETROL S.A.—Instituto Colombiano del Petróleo, Piedecuesta 681011, Colombia*

María Carolina Ruiz-Cañas − *ECOPETROL S.A.—Instituto Colombiano del Petróleo, Piedecuesta 681011, Colombia*

Henderson Quintero − *ECOPETROL S.A.—Instituto Colombiano del Petróleo, Piedecuesta 681011, Colombia*

Oscar E. Medina − *Grupo de Investigación en Fenómenos de Superficie - Michael Polanyi, Departamento de Procesos y Energía, Facultad de Minas, Universidad Nacional de Colombia, Sede Medellín 050034, Colombia;* orcid.org/0000-0002-1001-9456

Sergio H. Lopera − *Grupo de Investigación en Yacimientos de Hidrocarburos, Departamento de Procesos y Energía, Facultad de Minas, Universidad Nacional de Colombia, Sede Medellín 050034, Colombia*

Farid B. Cortés − *Grupo de Investigación en Fenómenos de Superficie - Michael Polanyi, Departamento de Procesos y Energía, Facultad de Minas, Universidad Nacional de Colombia, Sede Medellín 050034, Colombia;* orcid.org/0000-0003-1207-3859

Complete contact information is available at: https://pubs.acs.org/10.1021/acsomega.4c03517

Author Contributions

Hugo Alejandro García-Duarte: Conceptualization, Methodology, Validation, Writing−reviewing and editing; **María Carolina Ruiz-Cañas:** Conceptualization, Methodology, Validation, Writing−reviewing and editing; **Henderson Quintero:** Conceptualization, Methodology, Validation, Writing−reviewing and editing; **Oscar E. Medina:** Conceptualization; Data curation; Formal analysis; Investigation; Methodology; Software; Validation; Visualization; Writing - original draft. **Sergio H. Lopera:** Conceptualization, Methodology, Validation, Writing−reviewing and editing **Camilo A. Franco:** Conceptualization, Methodology, Formal analysis, Validation, Writing−reviewing and editing.

Funding

This research received no external funding.

Notes

The authors declare no competing financial interest.

ACKNOWLEDGMENTS

The authors gratefully acknowledge the invaluable support and resource contributions from the Universidad Nacional de Colombia and the Instituto Colombiano del Petróleo. Their provision of essential tools has been instrumental in facilitating the seamless execution and successful development of this study. The collaborative synergy between the authors and these esteemed institutions underscores the significance of their involvement, as they not only provided the necessary infrastructure but also played a pivotal role in shaping the trajectory of this research endeavor.

REFERENCES

(1) (a) Bera, A.; Babadagli, T. Status of electromagnetic heating for enhanced heavy oil/bitumen recovery and future prospects: a review. *Appl. Energy* **2015**, *151*, 206−226. (b) Franco, C.; Flórez, A.; Ochoa, M. Análisis de la cadena de suministros de biocombustibles en Colombia. *Rev. Dinám Sistemas* **2008**, *4*, 109−133.

(2) Vakhin, A. V.; Khelkhal, M. A.; Tajik, A.; Ignashev, N. E.; Krapivnitskaya, T. O.; Peskov, N. Y.; Glyavin, M. Y.; Bulanova, S. A.; Slavkina, O. V.; Schekoldin, K. A. Microwave radiation impact on heavy oil upgrading from carbonate deposits in the presence of nanosized magnetite. *Processes* **2021**, *9* (11), 2021.

(3) Galukhin, A.; Nosov, R.; Eskin, A.; Khelkhal, M.; Osin, Y. Manganese oxide nanoparticles immobilized on silica nanospheres as a highly efficient catalyst for heavy oil oxidation. *Ind. Eng. Chem. Res.* **2019**, *58* (21), 8990−8995.

(4) Shah, A.; Fishwick, R.; Wood, J.; Leeke, G.; Rigby, S.; Greaves, M. A review of novel techniques for heavy oil and bitumen extraction and upgrading. *Energy Environ. Sci.* **2010**, *3* (6), 700−714.

(5) Wilson, A. Nanoparticle Catalysts Upgrade Heavy Oil for Continuous-Steam-Injection Recovery. *Journal of Petroleum Technology* **2017**, *69* (3), 66−67.
(6) Wang, X.; Chen, J.; Zeng, J.; Wang, Q.; Li, Z.; Qin, R.; Wu, C.; Xie, Z.; Zheng, L. The synergy between atomically dispersed Pd and cerium oxide for enhanced catalytic properties. *Nanoscale* **2017**, *9* (20), 6643−6648.
(7) Giraldo, L. J.; Medina, O. E.; Ortiz-Perez, V.; Franco, C. A.; Cortés, F. B. Enhanced Carbon Storage Process from Flue Gas Streams Using Rice Husk Silica Nanoparticles: An Approach in Shallow Coal Bed Methane Reservoirs. *Energy Fuels* **2023**, *37* (4), 2945−2959.
(8) Medina, O. E.; Gallego, J.; Pérez-Cadenas, A. F.; Carrasco-Marín, F.; Cortés, F. B.; Franco, C. A. Insights into the Morphology Effect of Ceria on the Catalytic Performance of NiO-PdO/CeO2 Nanoparticles for Thermo-oxidation of n-C7 Asphaltenes under Isothermal Heating at Different Pressures. *Energy Fuels* **2021**, *35*, 18170.
(9) Afzal, S.; Ehsani, M. R.; Nikookar, M.; Roayaei, E. Effect of Fe2O3 and WO3 nanoparticle on steam injection recovery. *Energy Sources, Part A: Recovery, Utilization, and Environmental Effects* **2018**, *40* (3), 251−258.
(10) Hamedi Shokrlu, Y.; Babadagli, T. In-situ upgrading of heavy oil/bitumen during steam injection by use of metal nanoparticles: A study on in-situ catalysis and catalyst transportation. *SPE Reservoir Evaluation & Engineering* **2013**, *16* (03), 333−344.
(11) Franco, C.; Cardona, L.; Lopera, S.; Mejía, J.; Cortés, F. Heavy oil upgrading and enhanced recovery in a continuous steam injection process assisted by nanoparticulated catalysts. In *SPE improved oil recovery conference*; Society of Petroleum Engineers, 2016.
(12) Cardona, L.; Arias-Madrid, D.; Cortés, F.; Lopera, S.; Franco, C. Heavy oil upgrading and enhanced recovery in a steam injection process assisted by NiO-and PdO-Functionalized SiO2 nanoparticulated catalysts. *Catalysts* **2018**, *8* (4), 132.
(13) Cardona, L.; Medina, O. E.; Céspedes, S.; Lopera, S. H.; Cortés, F. B.; Franco, C. A. Effect of Steam Quality on Extra-Heavy Crude Oil Upgrading and Oil Recovery Assisted with PdO and NiO-Functionalized Al2O3 Nanoparticles. *Processes* **2021**, *9* (6), 1009.
(14) Medina, O. E.; Hurtado, Y.; Caro-Velez, C.; Cortés, F. B.; Riazi, M.; Lopera, S. H.; Franco, C. A. Improvement of steam injection processes through nanotechnology: An approach through in situ upgrading and foam injection. *Energies* **2019**, *12* (24), 4633.
(15) Medina, O. E.; Caro-Vélez, C.; Gallego, J.; Cortés, F. B.; Lopera, S. H.; Franco, C. A. Upgrading of extra-heavy crude oils by dispersed injection of NiO-PdO/CeO2±δ nanocatalyst-based nanofluids in the steam. *Nanomaterials* **2019**, *9* (12), 1755.
(16) Hosseinpour, M.; Fatemi, S.; Ahmadi, S. J. Catalytic cracking of petroleum vacuum residue in supercritical water media: impact of α-Fe2O3 in the form of free nanoparticles and silica-supported granules. *Fuel* **2015**, *159*, 538−549.
(17) Ancheyta, J.; Centeno, G.; Trejo, F.; Marroquin, G.; Garcia, J.; Tenorio, E.; Torres, A. Extraction and characterization of asphaltenes from different crude oils and solvents. *Energy Fuels* **2002**, *16* (5), 1121−1127. López, D.; Giraldo, L. J.; Salazar, J. P.; Zapata, D. M.; Ortega, D. C.; Franco, C. A.; Cortés, F. B. Metal oxide nanoparticles supported on macro-mesoporous Aluminosilicates for catalytic steam gasification of heavy oil fractions for on-site upgrading. *Catalysts* **2017**, *7* (11), 319.
(18) Cardona, L.; Arias-Madrid, D.; Cortés, F. B.; Lopera, S. H.; Franco, C. A. Heavy oil upgrading and enhanced recovery in a steam injection process assisted by NiO- and PdO-Functionalized SiO2 nanoparticulated catalysts. *Catalysts* **2018**, *8* (4), 132.
(19) (a) De la Cruz Flores, V. G. *Actividad y desactivación de Ni en HMS para el reformado de metano con CO2*, MS Thesis; Universidad Autónoma de Nuevo León, 2015. (b) Cortés, F. B.; Mejía, J. M.; Ruiz, M. A.; Benjumea, P.; Riffel, D. B. Sorption of asphaltenes onto nanoparticles of nickel oxide supported on nanoparticulated silica gel. *Energy Fuels* **2012**, *26*, 1725−1730.
(20) Haber, J.; Block, J. H.; Delmon, B. Manual of methods and procedures for catalyst characterization (Technical Report). *Pure Appl. Chem.* **1995**, *67*, 1257−1306.
(21) Franco, C.; Patiño, E.; Benjumea, P.; Ruiz, M. A.; Cortés, F. B. Kinetic and thermodynamic equilibrium of asphaltenes sorption onto nanoparticles of nickel oxide supported on nanoparticulated alumina. *Fuel* **2013**, *105*, 408−414.
(22) González Vera, O. F.; Mutiz, J. J.; Urresta Aragón, J. Síntesis y caracterización de catalizadores tipo Cu soportado en MgO, SiO2, ZnO y Al2O3 aplicados a la hidrogenólisis del glicerol. *Rev. ION* **2018**, *30*, 31−41.
(23) Medina, O. E.; Gallego, J.; Restrepo, L. G.; Cortés, F. B.; Franco, C. A. Influence of the Ce4+/Ce3+ Redox-couple on the cyclic regeneration for adsorptive and catalytic performance of NiO-PdO/CeO2±δ nanoparticles for n-C7 asphaltene steam gasification. *Nanomaterials* **2019**, *9* (5), 734.
(24) Medina, O. E.; Gallego, J.; Olmos, C. M.; Chen, X.; Cortés, F. B.; Franco, C. A. Effect of Multifunctional Nanocatalysts on n-C7 Asphaltene Adsorption and Subsequent Oxidation under High-Pressure Conditions. *Energy Fuels* **2020**, *34*, 6261.
(25) Medina, O. E.; Moncayo Riascos, I.; Heidari, S.; Acevedo, S. A.; Castillo, J.; Cortes, F. B.; Franco, C. A. Theoretical and experimental study of adsorption and catalytic reactivity of asphaltene fractions A1 and A2 over cubic NiO-PdO/CeO2 nanoparticles. *Fuel* **2024**, *375*, 132584.
(26) Bansal, V.; Krishna, G.; Chopra, A.; Sarpal, A. Detailed hydrocarbon characterization of RFCC feed stocks by NMR spectroscopic techniques. *Energy Fuels* **2007**, *21* (2), 1024−1029.
(27) García-Duarte, H. A.; Ruiz-Cañas, M. C.; Pérez-Romero, R. A. Innovative Experimental Design for the Evaluation of Nanofluid-Based Solvent as a Hybrid Technology for Optimizing Cyclic Steam Stimulation Applications. *Energies* **2023**, *16* (1), 373.
(28) Medina, O. E.; Gallego, J.; Arias-Madrid, D.; Cortés, F. B.; Franco, C. A. Optimization of the Load of Transition Metal Oxides (Fe2O3, Co3O4, NiO and/or PdO) onto CeO2 Nanoparticles in Catalytic Steam Decomposition of n-C7 Asphaltenes at Low Temperatures. *Nanomaterials* **2019**, *9* (3), 401.
(29) Nassar, N. N. Asphaltene adsorption onto alumina nanoparticles: kinetics and thermodynamic studies. *Energy Fuels* **2010**, *24* (8), 4116−4122.
(30) Lopes, A. M.; Wernert, V.; Sorbier, L.; Lecocq, V.; Denoyel, R. Adsorption of asphaltenes on multiscale porous alumina. *Adsorption* **2022**, *28* (7−8), 261−273.
(31) Shojaei, B.; Miri, R.; Bazyari, A.; Thompson, L. T. Asphaltene adsorption on MgO, CaO, SiO2, and Al2O3 nanoparticles synthesized via the Pechini-type Sol- Gel method. *Fuel* **2022**, *321*, 124136.
(32) Mbouopda Poupi, A. B.; Nchimi, K.; Nguele, R.; Iqbal, M.; Poulose, V.; Sasaki, K.; Saibi, H. An experimental study on the effect of alumina nanocomposites on asphaltene precipitation. *Petroleum Science and Technology* **2023**, 1−21.
(33) Nassar, N. N.; Hassan, A.; Pereira-Almao, P. Effect of surface acidity and basicity of aluminas on asphaltene adsorption and oxidation. *J. Colloid Interface Sci.* **2011**, *360* (1), 233−238.
(34) Guichard, B.; Gaulier, F.; Barbier, J.; Corre, T.; Bonneau, J.-L.; Levitz, P.; Espinat, D. Asphaltenes diffusion/adsorption through catalyst alumina supports-Influence on catalytic activity. *Catal. Today* **2018**, *305*, 49−57.
(35) Nassar, N. N.; Montoya, T.; Franco, C. A.; Cortés, F. B.; Pereira-Almao, P. A new model for describing the adsorption of asphaltenes on porous media at a high pressure and temperature under flow conditions. *Energy Fuels* **2015**, *29* (7), 4210−4221.
(36) Tang, F.-S.; Lin, R.-B.; Lin, R.-G.; Zhao, J. C.-G.; Chen, B. Separation of C2 hydrocarbons from methane in a microporous metal-organic framework. *J. Solid State Chem.* **2018**, *258*, 346−350. (a) Ji, D.; Zhong, H.; Dong, M.; Chen, Z. Study of heat transfer by thermal expansion of connate water ahead of a steam chamber edge in the steam-assisted-gravity-drainage process. *Fuel* **2015**, *150*, 592−601. (b) Huang, S.; Cao, M.; Cheng, L. Experimental study on

https://doi.org/10.1021/acsomega.4c03517
ACS Omega 2024, 9, 40511−40521

aquathermolysis of different viscosity heavy oil with superheated steam. *Energy Fuels* **2018**, *32* (4), 4850−4858. (c) Ageeb, A. A.; Al-siddig, M. H.; Nor-aldeen, M. R.; Soliman, M. S.; Ibrahim, I. H. The Influence of Steam Injection Volume on Sand and Oil Production in Cyclic Steam Stimulation (CSS) Wells, BSc Dissertation, Sudan University of Science and Technology, 2017.

(37) Lamonier, C.; Ponchel, A.; D'huysser, A.; Jalowiecki-Duhamel, L. Studies of the cerium-metal-oxygen-hydrogen system (metal= Cu, Ni). *Catal. Today* **1999**, *50* (2), 247−259.

(38) Pinc, W.; Yu, P.; O'Keefe, M.; Fahrenholtz, W. Effect of gelatin additions on the corrosion resistance of cerium based conversion coatings spray deposited on Al 2024-T3. *Surface & Coatings Technology* **2009**, *203*, 3533−3540.

(39) Yamaguchi, T.; Ikeda, N.; Hattori, H.; Tanabe, K. Surface and catalytic properties of cerium oxide. *J. Catal.* **1981**, *67* (2), 324−330.

(40) Alamolhoda, S.; Vitale, G.; Hassan, A.; Nassar, N. N.; Almao, P. P. Synergetic effects of cerium and nickel in Ce-Ni-MFI catalysts on low-temperature water-gas shift reaction. *Fuel* **2019**, *237*, 361−372.

(41) Wang, X.; Rodriguez, J. A.; Hanson, J. C.; Gamarra, D.; Martínez-Arias, A.; Fernández-García, M. In situ studies of the active sites for the water gas shift reaction over Cu- CeO2 catalysts: complex interaction between metallic copper and oxygen vacancies of ceria. *J. Phys. Chem. B* **2006**, *110* (1), 428−434.

(42) Diagne, C.; Idriss, H.; Kiennemann, A. Hydrogen production by ethanol reforming over Rh/CeO2-ZrO2 catalysts. *Catal. Commun.* **2002**, *3* (12), 565−571.

(43) Nassar, N. N.; Franco, C. A.; Montoya, T.; Cortés, F. B.; Hassan, A. Effect of oxide support on Ni-Pd bimetallic nanocatalysts for steam gasification of n-C7 asphaltenes. *Fuel* **2015**, *156*, 110−120.

(44) Lozano, M. M.; Franco, C. A.; Acevedo, S. A.; Nassar, N. N.; Cortés, F. B. Effects of resin I on the catalytic oxidation of n-C 7 asphaltenes in the presence of silica-based nanoparticles. *RSC Adv.* **2016**, *6* (78), 74630−74642.

(45) Medina, O. E.; Gallego, J.; Acevedo, S.; Riazi, M.; Ocampo-Pérez, R.; Cortés, F. B.; Franco, C. A. Catalytic Conversion of n-C7 Asphaltenes and Resins II into Hydrogen Using CeO2-Based Nanocatalysts. *Nanomaterials* **2021**, *11* (5), 1301.

(46) Marei, N. N.; Nassar, N. N.; Hmoudah, M.; El-Qanni, A.; Vitale, G.; Hassan, A. Nanosize effects of NiO nanosorbcats on adsorption and catalytic thermo-oxidative decomposition of vacuum residue asphaltenes. *Canadian Journal of Chemical Engineering* **2017**, *95* (10), 1864−1874.

(47) Marei, N. N.; Nassar, N. N.; Vitale, G.; Hassan, A.; Perez Zurita, M. J. Effects of the size of NiO nanoparticles on the catalytic oxidation of Quinolin-65 as an asphaltene model compound. *Fuel* **2017**, *207*, 423−437.

(48) Nassar, N. N.; Hassan, A.; Pereira-Almao, P. Thermogravimetric studies on catalytic effect of metal oxide nanoparticles on asphaltene pyrolysis under inert conditions. *J. Therm. Anal. Calorim.* **2012**, *110* (3), 1327−1332.

(49) Cano-Londono, N. A.; Medina, O. E.; Mozo, I.; Cespedes, S.; Franco, C. A.; Cortes, F. B. Viability of the Steam-based Extraction of Extra-Heavy Crude Oil using Nanoparticles: Exergy and Life-Cycle Assessment. *Energy* **2024**, *304*, 131929.

https://doi.org/10.1021/acsomega.4c03517
ACS Omega 2024, 9, 40511−40521